Ocean Engineering 315 (2025) 119799

Contents lists available at ScienceDirect

Ocean Engineering

journal homepage: www.elsevier.com/locate/oceaneng

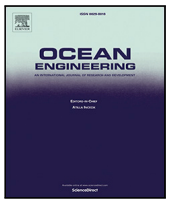

Research paper

Wave devouring propulsion for stabilizing floating wind turbine platform: Experimental study

Jingru Xing [a], Junxian Wang [a], Ashkan Matin [a], Ninad Prashant Vaidya [a], Liang Yang [a,*], Nicholas Townsend [b], Lei Zuo [c]

[a] Division of Energy and Sustainability, Cranfield University, UK
[b] Faculty of Engineering and Physical Sciences, University of Southampton, UK
[c] Department of Naval Architecture and Marine Engineering, University of Michigan, Ann Arbor, MI, 48109, USA

ARTICLE INFO

Keywords:
Flapping foil
Wave-induced propulsion
Semi-submersible platform
Offshore wind

ABSTRACT

Wave Devouring Propulsion (WDP) is a green propulsion method that uses submerged foils to convert wave energy into thrust, serving both as an auxiliary propulsion system and as a stabilizer for maritime structures. This study highlights WDP's effectiveness in improving stability for semi-submersible offshore wind turbine platforms. Experiments on a 1:100 scaled model in regular and irregular head wave conditions were conducted in both free-floating conditions, and with a mooring system to validate WDP's effectiveness. Results show that the integrated foil design reduced mooring line tension by 41.07% compared to the design without foils in specific scenarios, suggesting a promising avenue for future research and application.

1. Introduction

Currently, the Levelized Cost of Energy (LCOE) for floating offshore wind significantly exceeds that of fixed offshore wind by more than threefold (Alvik, 2023). This discrepancy is attributed primarily to the challenges posed by the excessive and violent motions experienced by floating wind platforms. These motions, triggered by severe operational and/or survival storm conditions, exert considerable strain on the mooring systems and induce large motions and vibrations in the turbines. To mitigate these issues, this study proposes the application of Wave Devouring Propulsion (WDP) techniques for platform stabilization. To enhance the stability of Floating Offshore Wind Turbines (FOWTs), three principal design philosophies are generally employed: buoyancy stability (as seen in barge-type platforms), ballast stability (utilized in spar-type platforms), and mooring stability (applied in tension-leg and semi-submersible platforms) (Chuang et al., 2021; WindEurope, 2017; Du, 2021). These design concepts is illustrated in Fig. 1. Various platform designs are paired with corresponding mooring system configurations to achieve stability, taking into account the environmental conditions of the site. The mooring systems hold particular significance for semi-submersible platforms, which are among the most prevalent forms of FOWT (Roddier et al., 2010).

Existing technologies employed for stabilizing offshore platforms in the industry fall into three main categories. The first category focuses on increasing the hydrodynamic damping of the floating platform. For example, barge-type floating platforms frequently incorporate a moonpool – a central opening within the hull – intended to dissipate energy and lessen the effects of wave-induced motions (Chuang et al., 2021; Tan et al., 2021). An illustration of this is the Floatgen project, a 2 MW floating wind turbine demonstrator in France, facilitated by Ideol, which employs a moonpool (depicted in Fig. 2(a)). Similarly, semi-submersible platforms might feature heave plates affixed to the columns' bottoms, as shown in Fig. 2(b), introducing added hydrodynamic damping forces through vortex generation at the edges (Roddier et al., 2010; Lopez-Pavon and Souto-Iglesias, 2015). However, both moonpools and heave plates have shown limitations in efficiently reducing platform drift caused by waves and currents, leading to increased axial tension in the mooring lines.

The second category to reducing mooring loads involves the use of Thruster-Assisted Position Mooring (TAPM) systems or spring-like connectors. TAPM systems, illustrated in Fig. 2(c), are prevalent in the oil and gas sector for reducing forces on mooring lines and platform offset (Ma et al., 2019). Besides offering standard Dynamic Positioning (DP) functionalities, a TAPM system incorporates a mooring system that delivers passive restoring forces and moments, leveraging the advantages of both passive mooring and active DP systems. Despite their efficacy, the use of TAPM systems with DP thrusters is marked by substantial energy consumption, along with elevated operational and maintenance expenses. Moreover, spring-like connectors, referenced in Fig. 2(d), designed to integrate into the mooring line, aim to mitigate

* Corresponding author.
E-mail address: liang.yang@cranfield.ac.uk (L. Yang).

https://doi.org/10.1016/j.oceaneng.2024.119799
Received 13 September 2024; Received in revised form 31 October 2024; Accepted 13 November 2024
Available online 21 November 2024

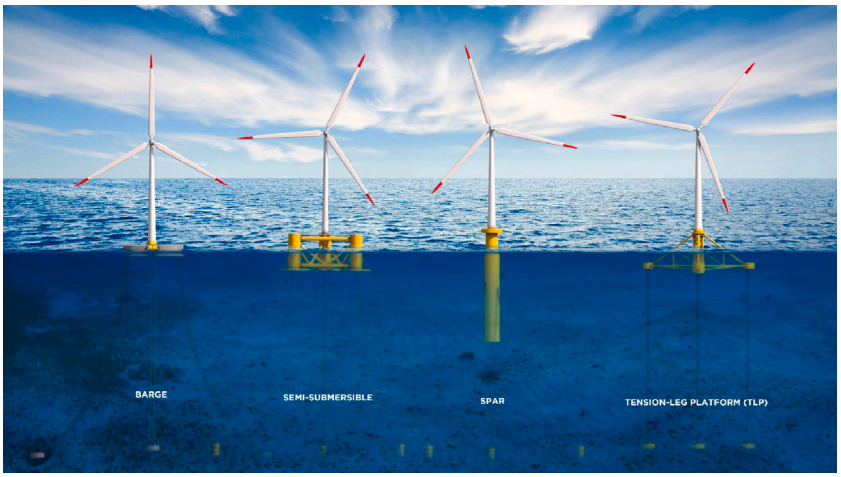

Fig. 1. Comparative structures of offshore wind turbine foundations (WindEurope, 2017).

(a) Moonpool of Floatgen [10]

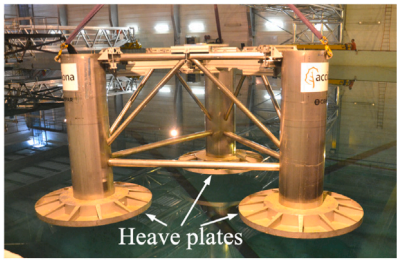

(b) Heave plates under semi-submersible platform [11]

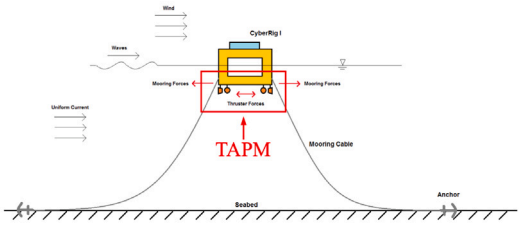

(c) TAPM systems [12]

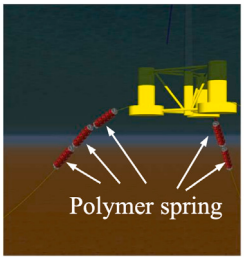

(d) Spring-like connectors [13]

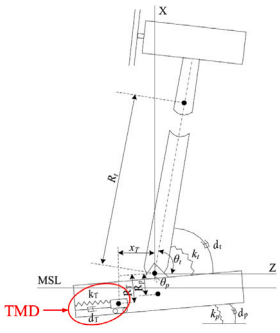

(e) TMD [14]

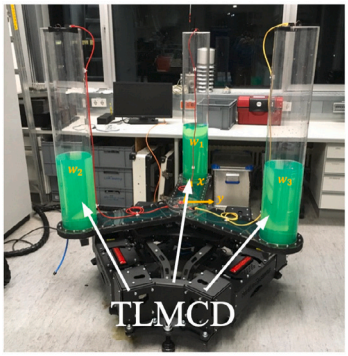

(f) TLMCD [15]

Fig. 2. Different types of offshore platform stabilization technologies (Ideol, 2022; Bezunartea-Barrio et al., 2020; Bjørneset, 2014; Johnston, 2018; Yang et al., 2019; Yu et al., 2023).

peak mooring loads (Aryawan et al., 2023). Nonetheless, the integration of such connectors introduces a heightened risk of wear and tear on moving parts, potentially compromising system reliability over time.

The third category focuses on vibration damping systems designed to reduce the motion of the platform by absorbing and dissipating energy. An example of this is the use of Tuned Mass Dampers (TMDs) (Yang et al., 2019), which are systems that use a secondary mass that oscillates out of phase with the platform to counteract unwanted vibrations, as shown in Fig. 2(e). Similarly, Tuned Liquid Multi-Column Dampers (TLMCDs) are employed in FOWTs to provide bi-directional

damping. TLMCDs in Fig. 2(f) use the movement of liquid within multiple columns to reduce the platform's response to wave and wind-induced motions (Yu et al., 2023). Both TMDs and TLMCDs offer significant potential in enhancing platform stability by targeting and mitigating specific resonant frequencies that contribute to excessive motion. However, the design and implementation of these systems require careful consideration of the platform's dynamic characteristics to achieve optimal performance.

The aforementioned methods, while innovative, exhibit certain limitations in stabilizing offshore platforms. In this context, WDP is a novel solution that promises a more effective approach to overcoming these challenges. Inspired by the natural movements of aquatic animals, particularly whales, WDP utilizes flapping foils to convert wave energy for thrust generation (Weinblum, 1954; Isshiki and Murakami, 1983; Wang et al., 2023, 2024; Chan et al., 2024; Wu et al., 2020; Bowker and Townsend, 2022; Bowker et al., 2020). The concept of WDP was first proposed by Weinblum and Georg in the 1950s (Weinblum, 1954), who developed a theoretical method to study the seaworthiness of foils. Isshiki and Murakami (1983) further conducted a series of experimental and theoretical studies on the WDP mechanism, particularly focusing on a foil placed in waves with a shallow draft. The results indicated that the forward speed and heave amplitude of a passive foil tend to rise in short waves and fall in long waves as the wavelength increases, providing valuable insights into the dynamic response of foils under different wave conditions. Bowker et al. (2015), Bowker and Townsend (2022) and Bowker et al. (2020) investigated the performance of an Autonomous Surface Vehicle (ASV) equipped with two passive foils submerged at the bow and stern under head wave conditions in a towing tank. Their experiments demonstrated that this innovative system could achieve either propulsion or power generation, with an average output of 1 W and a peak output of 4 W.

Building on these foundational studies, the application of WDP to offshore platforms offers significant potential for enhancing stability. By integrating these foils with offshore platforms, the motion of the foils and the movement of the platform in the marine environment translates the kinetic energy of waves into stabilizing forces for the platforms. Distinguished by its passive operation, WDP requires no external power sources or feedback mechanisms. This innovative method offers a compelling advantage by significantly reducing platform vibrations and mooring line loads, all while necessitating minimal maintenance.

While WDP technology has attracted considerable interest from both the scientific and commercial sectors, its application has predominantly been in the context of marine vehicles, such as Unmanned Surface Vehicles (USVs) (Hine et al., 2009; Johnston and Poole, 2017; AutonautusV, 2023) and ships (Terao, 2009; Bøckmann et al., 2018). Notable among these is the Suntory Mermaid II (Terao, 2009), a wave-powered vessel that achieved a landmark trans-Pacific voyage from Honolulu. Despite these successful implementations, the integration of WDP technology in offshore platforms remains a largely uncharted domain Xing and Yang (2023), presenting a promising avenue for future research and development in marine propulsion systems. Here, it is worth highlighting a study by Yoshida et al. (2018), who also attached the WDP to the platform. However, their approach differs significantly from the present study. While both studies attach the plate to the platform's lower beam, Yoshida et al. (2018) used a flat plate, whereas this research employs a NACA0030 foil shape, emphasizing the influence of the foil shape and pitch angle over the motion itself. Furthermore, Yoshida et al.'s (2018) platform was not a standardized semi-submersible platform, and their experiments were conducted entirely under free-floating conditions, without considering the advantages of WDP for mooring lines. Their focus was mainly on the changes in platform position due to wave angle variations, monitored via video camera tracking, without addressing changes in heave, pitch, or drift speed.

This study innovatively explores the utilization of WDP for semi-submersible platforms, employing scaled-down models within a wave tank under regular and irregular wave conditions. The research examines the configuration of foils attached to the platform, with free-floating tests and moored tests to investigate and validate the effectiveness of WDP. Specifically, this study aims to experimentally achieve quantifiable improvements in platform stability, such as reducing drift speed and mooring line tension by a measurable percentage under dynamic wave conditions.

The paper is organized as follows: Section 2 provides an in-depth description of the experimental arrangement, detailing the scaled-down model and foil plates, the setup of the wave tank, and the specific wave conditions. Section 3 investigates the impact of different foil pitch angles under varying wave conditions. Further, in Section 4, the proposed design is validated by distinct the mooring line tension reduction. Finally, Section 5 summarizes the conclusions of the study.

2. Experimental setup

2.1. Platform model

This study adopts semi-submersible platforms as the chosen model, a prevalent type of offshore wind platform, with its layout based on the OC5 DeepCwind floating system (Robertson et al., 2017). To ensure the platform's behavior in water closely mimics that of its real-life prototype, it was scaled down with the scale factor of 100 ($\lambda = 100$).

Fig. 3 displays the 3D CAD model of the platform along with a photograph of its placement in the tank. The wave propagates along the positive x-direction. The platform model is semi-submerged in the tank with calm water, and its draft, which is the depth of the platform below the still water level (SWL), measures 0.2 m. The platform consists of one main column at the center and three offset columns. Each offset column is composed of a 5 mm thick acrylic cylinder with a polyethylene foam offset base. These three offset columns are arranged in the shape of an equilateral triangle and are connected to the main column through aluminum hollow beams. Table 1 provide a comprehensive summary of the platform model's dimensions.

2.2. Foil and parameters

The study utilizes NACA type foils, specifically NACA0030, as the chosen foil geometry. These symmetrical foils are characterized by their chord length c, defined as the straight line connecting the leading to the trailing edge, which for symmetric foils coincides with the mean camber line. Depending on the wake patterns it produces, a foil can generate either a drag or thrust force. When a von Kármán vortex street (vK) forms, the flow velocity in the wake is slower compared to the approaching or ambient flow, causing the foil to enter a drag-dominated regime. However, when the wake vortices align at the trailing edge of the foil, a neutral condition occurs where the wake velocity matches the ambient flow velocity, resulting in no net thrust or drag. As these conditions progress further, thrust can be generated. When a reversed von Kármán vortex street (RvK) develops, it accelerates the flow behind the foil, leading to thrust generation. The formation of a reversed RvK wake marks the beginning of the transition from drag to thrust. Nevertheless, there is a delay in reaching effective thrust production, as the small velocity increase cannot yet overcome the foil's inherent drag, as well as the effects of velocity fluctuations and pressure differences (Lagopoulos et al., 2019; Streitlien and Triantafyllou, 1998; Ramamurti and Sandberg, 2001; Bohl and Koochesfahani, 2009). Fig. 4 illustrates the three fundamental wake patterns. In other words, the thrust-generating effect of the foil is not universally guaranteed; it only emerges under specific wake conditions, such as the formation of a reversed von Kármán vortex street. This makes it essential to investigate the potential of integrating this technology into semi-submersible wind turbine platforms. Understanding the conditions that facilitate effective thrust generation is crucial for optimizing the stability and efficiency of offshore wind turbines.

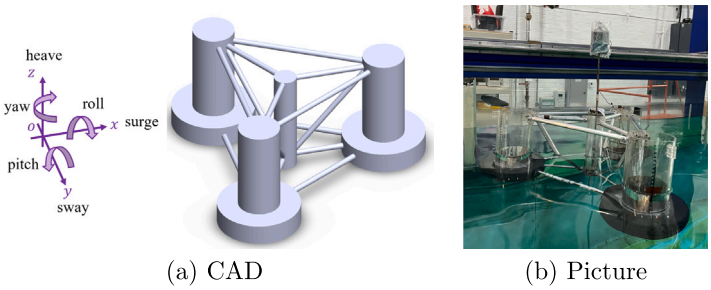

Fig. 3. 3D CAD model and photograph of the semi-submersible platform placed in the tank.

Table 1
The dimensions of the platform model.

Properties	Units	Scaled model	Full model	Scaling factor (1:100)
Depth of platform base below SWL (draft)	m	0.2	20	λ
Elevation of main column below SWL	m	0.1	10	λ
Elevation of offset columns above SWL	m	0.12	12	λ
Height of offset columns	m	0.26	26	λ
Height of foam bases	m	0.06	6	λ
Depth to bottom beams below SWL	m	0.14	14	λ
Diameter of main column	m	0.065	6.5	λ
Diameter of offset columns	m	0.12	12	λ
Diameter of foam bases	m	0.24	24	λ
Diameter of beams	m	0.016	1.6	λ
Thickness of beams	m	0.0015	0.15	λ
Distance between each offset columns	m	0.5	50	λ
Platform mass including ballast	kg	12.919	12 919 000.00	λ^3

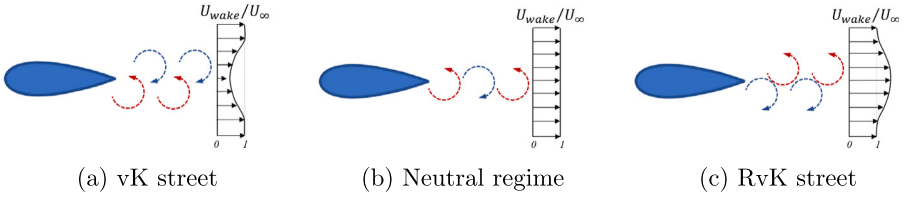

Fig. 4. The illustration for the drag-to-thrust wake transition of the flapping foil.

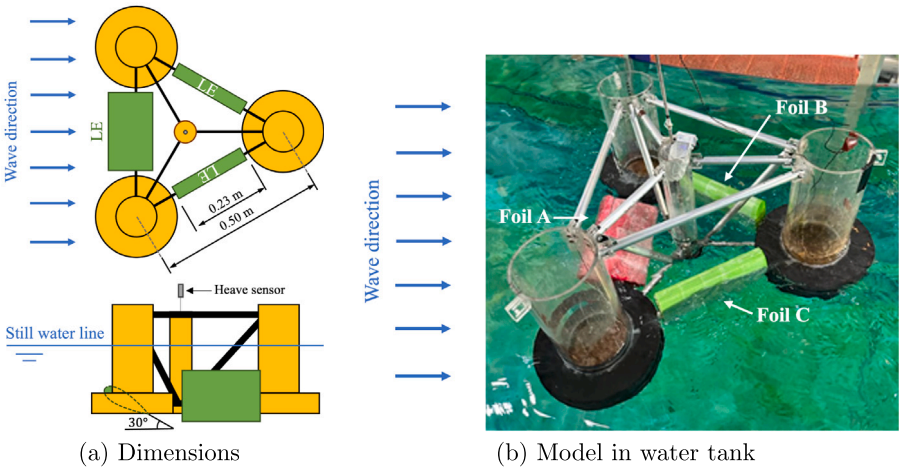

Fig. 5. The dimensions of the design model (semi-submersible platform with 3 foils).

Fig. 5 shows the position of the foils on the platform. Three foils are connected to the lower beams of platform.

For the experiments, NACA0030 foil plates with a chord length c of 150 mm and a span s of 230 mm were fabricated using 3D printing and PLA plastic (see Fig. 6(b)). All tests mentioned in this study use rear hole plates, while front hole plates are used only in a small subset of experiments investigating the influence of the pitch angles, as detailed in Section 3.2. These foil plates have a density of 314.6 kg/m^3. They serve exclusively as the 'foil' elements, maintaining the platform's intended behavior while effectively fulfilling their role in WDP.

The interaction between a moving foil and the oncoming flow is described through the non-dimensional Strouhal numbers. The peak-to-peak oscillating amplitude, A, of the foil's trailing edge and it is oscillating frequency, f, are normalized with the characteristic flow

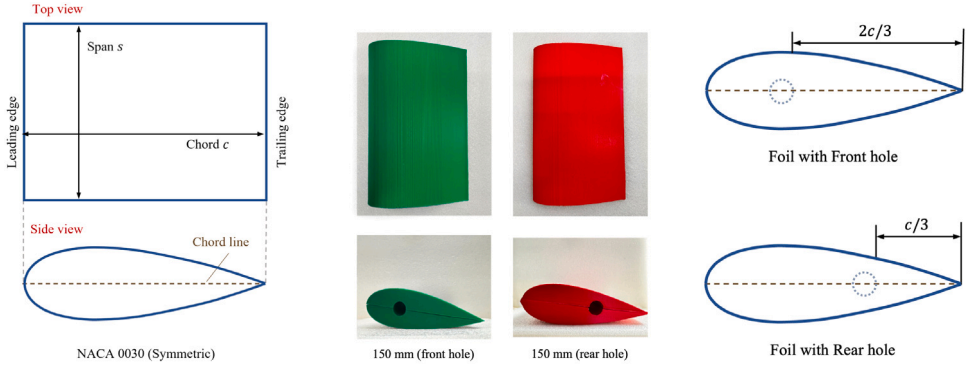

(a) Foil characteristics (b) Product of 3D printed foils (c) Hole position

Fig. 6. NACA0030 foil plates used for the study.

velocity, U_∞, for estimating St_A, Eq. (1) (Triantafyllou et al., 1991).

$$St_A = \frac{fA}{U_\infty} \tag{1}$$

It is assumed that the direction of U_∞ is always aligned with the heading wave direction. The oscillating amplitude A is often taken as the width of the wake.

2.3. The assemble of platform and foil

Fig. 5 illustrates the appearance after installing three foil plates along with the dimensions of the model. The foils are positioned on the lower beams between two foam offset bases. One of the primary motivations for this placement is the understanding that the closer the foil is to the water surface, the more wave energy is available for conversion, resulting in a greater thrust (Isshiki and Murakami, 1984; Xing and Yang, 2023). Additionally, the beam provides a convenient point of attachment for the foil, and its surrounding space remains unobstructed, ensuring the platform's original design remains intact. To capture heave motion data, the GoDirect Force and Acceleration Sensor is firmly situated at the platform's central screw (see in Fig. 5(a), the grey rectangular part in the side view). The sensor measures force from ±50 N with a resolution of 0.01 N, acceleration up to ±16 g with a resolution of 0.01 g, and rotational motion with a resolution of 0.1°. It supports a maximum sampling rate of 200 Hz. For this experiment, data was sampled at 50 Hz to accurately capture dynamic responses. The sensor was calibrated using Go Direct software before each test.

For clear delineation, the foils, placed fixed in three distinct positions, are individually named. The foil facing the head wave is designated as Foil A, illustrated in red in Fig. 5(b). The other two offset foils are denoted as Foil B and Foil C, portrayed in green in Fig. 5(b). Foils B and C were maintained in a vertical orientation throughout the experimental tests in this study, meaning that when stationary, the offset foils B and C were perpendicular to the water surface. This configuration was chosen to primarily focus on the influence of the frontal foil (Foil A). Additionally, using three foils allows for consideration of wave impacts from various directions.

2.4. Wave condition

The Cranfield University PSE lab wave tank/towing tank has three flaps as the wave generator on one end, and a metal beach as wave absorption on the other end. The wave tank frame has a size of 30 m long, 1.5 m wide and 1.5 m water depth. Table 2 presents the pitch angles and wave conditions used in all scenarios for this experiment.

2.4.1. Regular wave condition

Regular wave is selected as the wave condition. The flow conditions, in the form of horizontal and vertical velocity, are calculated using linear wave theory and specifically:

$$u(x,z,t) = \frac{\pi H}{T}\frac{\cosh[k(z+d)]}{\sinh(kd)}\cos(kx-\omega_w t) \tag{2a}$$

$$v(x,z,t) = \frac{\pi H}{T}\frac{\sinh[k(z+d)]}{\sinh(kd)}\sin(kx-\omega_w t) \tag{2b}$$

where, u and v are the instantaneous horizontal and vertical particle velocities at (x, y) location, H is the wave height, T is the wave period, d is the water depth, $k = \frac{2\pi}{\lambda}$ is the wave number, $\omega_w = \frac{2\pi}{T}$ is the angular wave frequency, and λ the wavelength calculated with the linear dispersion equation, Eq. (3).

$$\lambda = \frac{gT^2}{2\pi}\tanh(kd) \tag{3}$$

To assess the performance under different wave conditions, appropriate wave conditions are selected based on the St_A number, refer to Eq. (1). For the passive running test, the platform's motion is influenced by the waves. The model oscillates up and down in sync with the wave frequency, and the wave height H can serve as an estimate for the platform's heave amplitude. This is because, under wave influence, the vertical displacement of the platform closely follows the wave height. While other factors like inertia and damping might affect the actual amplitude, H provides a reasonable first approximation. Thus, in Eq. (1), the oscillating frequency f can be reasonably replaced with wave frequency f_w and the oscillating amplitude A can be approximated with the wave height H.

Regarding the characteristic flow velocity, U_∞, five choices are available: wave celerity, horizontal and vertical velocities at the foil's initial submerged location (z = −0.17 m), or the horizontal and vertical velocities at the still water level (z = 0). For the designed model (a combination of WDP and platform), the foil experiences varying flow conditions due to wave-induced kinematics at different depths. The selection of the characteristic velocity should be based on the foil's motion, as the study focuses on the foil's WDP capability. Therefore, choosing the horizontal and vertical velocities at the foil's initial submerged location (z = −0.17 m) is more appropriate than simply using the wave celerity or velocities at the surface. Additionally, the horizontal velocity magnitude is larger than the vertical velocity and acts over the foil surface, producing desired effects such as a vortex street. The foil's trajectory, induced by waves, is smaller than that of the wave particles at z = –0.17 m. At this depth, the wave particle velocity represents the maximum velocity the foil can reach. Therefore, U_∞ can be expressed as the maximum horizontal velocity at the initial submerged location of the foil (z = −0.17 m), denoted as U_{umax}, as shown in Eq. (4a). Finally, Eq. (1) is presented in a wave-based form as Eq. (4b).

$$U_u = \frac{\pi H}{T}\frac{\cosh[k(z+d)]}{\sinh(kd)} \tag{4a}$$

$$St_A = \frac{f_w H}{U_{umax}} \tag{4b}$$

Table 2
Test matrix for all conditions.

Pitch angle (°)	Type	Water depth d (m)	Height H (m)	Frequency f (Hz)	Wave period T (s)	Wavelength λ (m)
Free-floating tests						
180	Airy	1.50	0.15	0.65	1.54	3.65
150	Airy	1.50	0.15	0.65	1.54	3.65
90	Airy	1.50	0.15	0.65	1.54	3.65
30	Airy	1.50	0.15	0.65	1.54	3.65
15	Airy	1.50	0.15	0.65	1.54	3.65
0	Airy	1.50	0.15	0.65	1.54	3.65
−15	Airy	1.50	0.15	0.65	1.54	3.65
−30	Airy	1.50	0.15	0.65	1.54	3.65
−90	Airy	1.50	0.15	0.65	1.54	3.65
−150	Airy	1.50	0.15	0.65	1.54	3.65
−180	Airy	1.50	0.15	0.65	1.54	3.65
30	Airy	1.50	0.15	0.45	2.22	6.79
30	Airy	1.50	0.15	0.50	2.00	5.78
30	Airy	1.50	0.15	0.55	1.82	4.95
30	Airy	1.50	0.15	0.60	1.67	4.25
30	Airy	1.50	0.15	0.65	1.54	3.65
30	Airy	1.50	0.15	0.70	1.43	3.18
30	Airy	1.50	0.15	0.75	1.33	2.76
30	Airy	1.50	0.15	0.80	1.25	2.44
30	Airy	1.50	0.15	0.85	1.18	2.17
30	Airy	1.50	0.15	0.90	1.11	1.92
30	Airy	1.50	0.15	0.95	1.05	1.72
30	Airy	1.50	0.15	1.00	1.00	1.56
Moored tests						
30	Airy	1.50	0.02	0.65	1.54	3.65
30	Airy	1.50	0.04	0.65	1.54	3.65
30	Airy	1.50	0.06	0.65	1.54	3.65
30	Airy	1.50	0.08	0.65	1.54	3.65
30	Airy	1.50	0.10	0.65	1.54	3.65
30	Airy	1.50	0.12	0.65	1.54	3.65
30	Airy	1.50	0.14	0.65	1.54	3.65
30	Airy	1.50	0.16	0.65	1.54	3.65
30	Airy	1.50	0.18	0.65	1.54	3.65
30	Airy	1.50	0.20	0.65	1.54	3.65
Pitch angle	Type	Water depth	Significant wave height	Peak frequency	Peak period	Peakedness parameter
30	JONSWAP	1.50	0.125	0.798	1.253	3.30

Anderson (1996) reported optimum thrust generation for $0.2 < St_A < 0.5$, and this range was further supported by simulations conducted by Xing et al. (2024). Read et al. (2003) not only reinforced Anderson's conclusions but also broadened the range of exploration up to an St_A value of 0.6. Given this confluence of findings, our study strategically focuses on wave conditions with a frequency of 0.65 Hz and a height of 0.15 m. These conditions correspond to an St_A value of 0.42, placing it squarely within the empirically established optimal range, thus offering a promising avenue for identifying conditions of peak efficiency.

2.4.2. Irregular wave condition

The experiment utilized irregular waves, specifically JONSWAP spectrum waves, to replicate realistic ocean conditions. The wave parameters were modeled based on data from the northern region of Scotland around the Orkney Islands, extending towards the Atlantic Ocean. These wave conditions correspond to the 50-year return period data collected by UK ocean surveys (Bricheno et al., 2015). Fig. 7 illustrates the significant wave height (H_s) of this region, which ranges between 10 m and 15 m. For the present experiment, a wave height of 12.5 m was chosen as a representative value. The corresponding wave period (T_s) was calculated using Morrison's equation (Arany et al., 2017), with g representing gravitational acceleration:

$$T_s = 11.1\sqrt{\frac{H_s}{g}} \tag{5}$$

For the experiment, the peakedness parameter (γ) used was set to 3.3, which is a standard value commonly used in irregular wave studies to approximate real sea states. Thus, the parameters were $H_s = 12.5$ m, $T_s = 12.53$ s, and $\gamma = 3.3$.

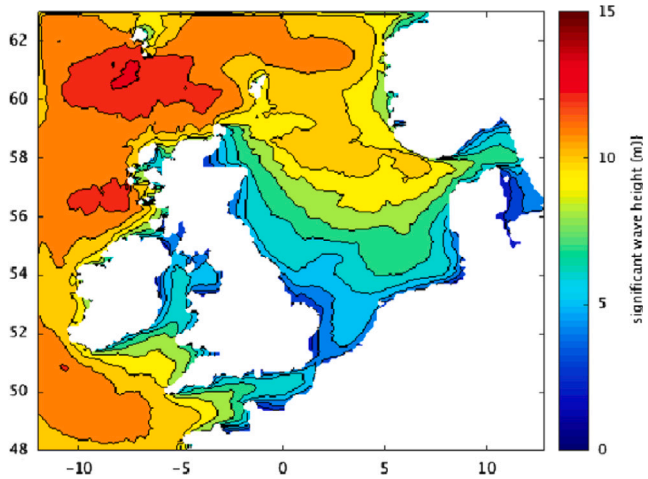

Fig. 7. 50-year significant wave height at North Sea and north Atlantic Sea.

The scaling technique employed was Froude scaling, ensuring consistency with the platform scaling. According to Froude's law, the significant wave height was scaled down to a ratio of 1:100, and the wave period was scaled down to a ratio of 1:10. Therefore, the final scaled wave conditions used were $H_s = 0.125$ m, $T_s = 1.253$ s, and $\gamma = 3.3$.

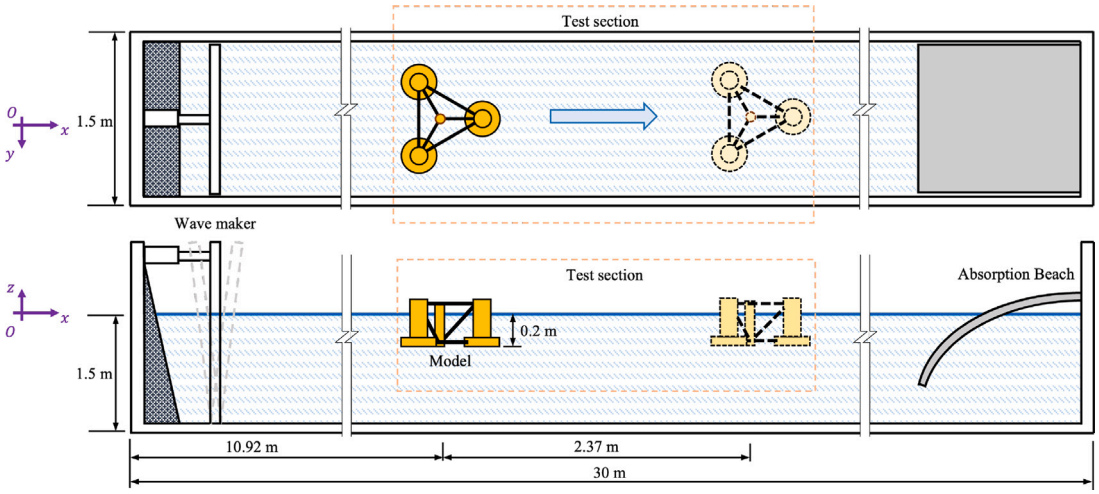

Fig. 8. The schematic diagram of the wave tank setup (without 3-foil setup).

These specific conditions were selected as they represent significant wave conditions in the North Atlantic, similar to the 50-year extreme conditions observed off the east coast of the UK towards the North Sea.

3. Free-floating tests

Free-floating Tests concentrate on pitch angle of the front foil and wave conditions influence to find the optimal design for enhancing platform stability.

3.1. Wave tank setup

The free-floating experimental setup is shown in Fig. 8. The center of the platform is positioned 10.92 m away from the side of the tank where waves are generated. The test distance is the spacing between the two tank pillars (not shown in the picture), which is 2.37 m. In the experiments, the wave maker generates regular waves through repeated oscillations according to set parameters. The free-floating platform, when impacted by these waves, drifts in the positive x-direction, deviating from its starting position. This section examines the drift velocity of the platform under different pitch angles and varying wave conditions.

Under regular wave conditions, the average drifting speed of the models was recorded within the test section with the drifting distance of 2.37 m. The average speed was determined by recording the time taken for each pass through the test section. The speed was then calculated using the formula: speed = distance/time. To minimize the influence of 3D effects, only tests where the model maintained a straight-line drift in the test section without any deviation or offset were considered valid. To ensure the reliability of the findings, results were averaged from three valid trials for each configuration.

3.2. Effect of pitch angle

In this section, the study use 3 foils as the foundational setup, see in Fig. 5. The primary objective is to identify the optimal design for the "WDP+platform" by altering the pitch angle of the foil oriented towards the wavefront. A comprehensive range of pitch angles of Foil A was tested, spanning from −180° to +180°, specifically at: −180°, −150°, −90°, −30°, −15°, 0°, 15°, 30°, 90°, 150°, and 180°, see Fig. 9. This extensive range allows for an in-depth analysis of the system's response across different attack angles. Due to spatial constraints at the foil's rear upon its installation on the platform, a full 150 mm rear-hole foil flip was not feasible. As a result, pitch angles of ±150° and ±180° employed a front hole, while the range from −90° to 90° utilized a rear hole foil. The tests were conducted with a wave height of 0.15 m and a frequency of 0.65 Hz. Under free-floating conditions, the model was tested for variations in drifting speed and heave acceleration changes under head waves at different pitch angles of Foil A. Each specific configuration was tested three times, with the results subsequently averaged to ensure reliability and robustness.

These results, along with the percentage reduction in drifting speed compared to the platform without foils, are summarized in Fig. 10. Compared to the no-foil baseline, all pitch angles in this setup significantly reduced the drifting speed. Within the range of −30° to 30°, there is a marked reduction in drifting speed, with optimal performance observed at pitch angle = 30°, recording a speed reduction of 60.04% compared to the non-foil platform. Conversely, for obtuse pitch angle (±90°, ±150°, ±180°), the foil exhibits limited effectiveness in influencing the system's speed. This reveals that, under conditions where the pitch angle is obtuse, the contribution of the foil to system performance is minimal or negligible.

Fig. 11 presents a comparative analysis of heave acceleration. Data collection began as the wave passed over the platform, during which the platform maintained a stable heave motion. Heave acceleration was recorded over 18 wave periods, capturing the acceleration for each cycle. The results are summarized and depicted in Fig. 11. Overall, there is a significant reduction in heave acceleration, generally hovering between a reduction of 12% to 15%. However, an anomaly is observed at pitch angle = 90°. Specifically, when all three foils are positioned vertically with their leading edges (LE) facing upwards, the decrease in heave acceleration is recorded at −3.85%. This implies that instead of mitigating the heave motion, this configuration inadvertently amplifies it. The presence of WDP generally leads to a reduction in the platform's heave amplitude, which is a positive outcome. This reduction might also be attributed to an added mass effect similar to that of a heave plate. Regardless of the pitch angle, the reduction in heave acceleration remains relatively consistent, suggesting that the benefits of reduced heave are similar across different pitch angle configurations. Therefore, the primary consideration in selecting the optimal design is the impact on drifting speed, which has a more significant influence.

3.3. Effect of wave frequency

Given the nature of real-world marine environments, it is imperative to evaluate the platform's performance under varying wave conditions. Prior research has shown that among various configurations, the three-foil setup – with one foil set at a pitch angle of 30 degrees (referred to as Foil A) and the other two being vertical foils (Foil B and C) – exhibits superior efficacy. This section aims to identify the precise wave conditions where this configuration demonstrates peak performance.

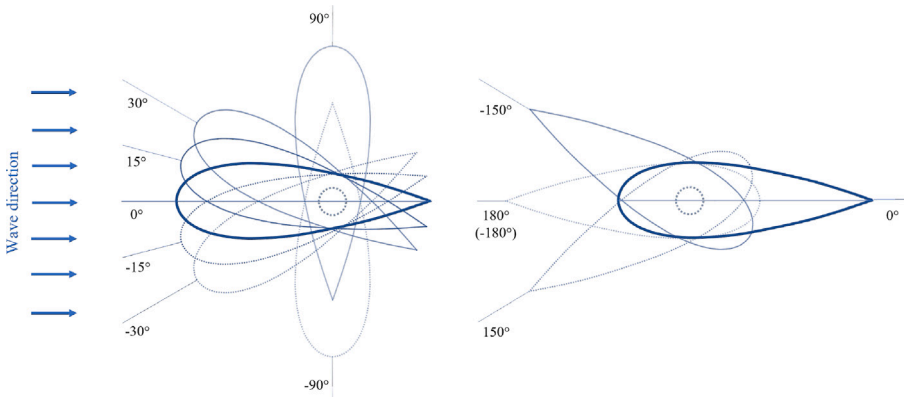

Fig. 9. The selection of pitch angle for front foil (Foil A).

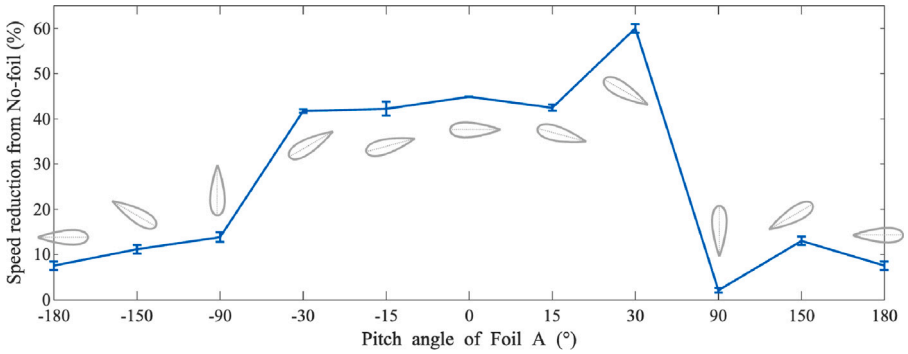

Fig. 10. Comparison of drifting speeds: varied pitch angle of Foil A with vertical Foil B and C. (The *y*-axis represents the drift speed reduction of the WDP+platform model compared to the No-foil setup, expressed as a percentage, and the *x*-axis shows the different pitch angles. The grey foil icon illustrates the actual rotational position of Foil A).

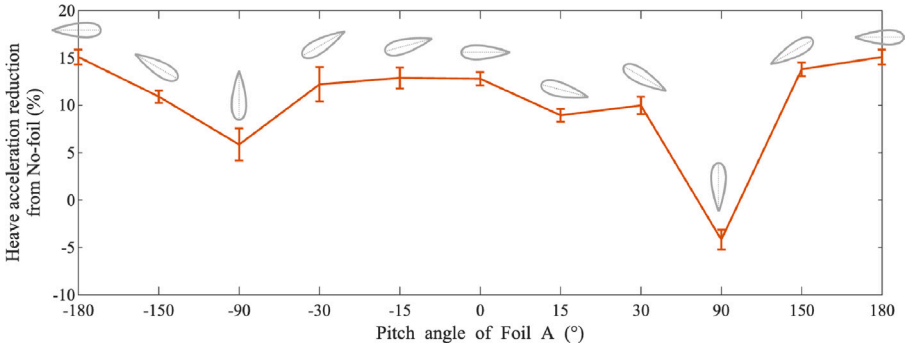

Fig. 11. Comparison of heave acceleration: varied pitch angle of Foil A with vertical Foil B and C. (The *y*-axis represents the heave acceleration reduction of the WDP+platform model compared to the No-foil setup, expressed as a percentage, and the *x*-axis shows the different pitch angles. The grey foil icon illustrates the actual rotational position of Foil A).

To ensure uniformity in the tests, a wave height of 0.15 m, as outlined in previous sections, was consistently maintained. The wave frequencies were methodically adjusted, ranging from 0.45 to 1 Hz, with increments of 0.05 Hz. To enhance measurement precision, a test distance of 1 m was chosen for determining the platform's drifting speed. Opting for a shorter test distance of 1 m, instead of the 2.37 m used in other sections, minimized inaccuracies due to wave interactions near the tank's shoreline. This is especially relevant when testing high-frequency waves which might cause backflow, subsequently pushing the platform in the opposite direction and causing inconsistent and extended floating duration.

Results, as depicted in Fig. 12, show that as wave frequencies increase, the platform's drifting speed also escalates. At these elevated frequencies, the platform encounters more frequent propelling forces, explaining this trend. This emphasizes the need to understand how different wave conditions can affect the platform's stability, especially in offshore environments where wave dynamics are constantly in flux.

4. Moored tests

This section examines the effectiveness of WDP in enhancing the structural stability of offshore platforms, with a specific focus on its interaction with mooring systems. The study assesses the potential of WDP in reducing tension on mooring lines, thus contributing to overall stability.

4.1. Wave tank and mooring system setup

The design includes three adjustable NACA0030 foils, each with a 150 mm chord length, integrated between the semi-submersible

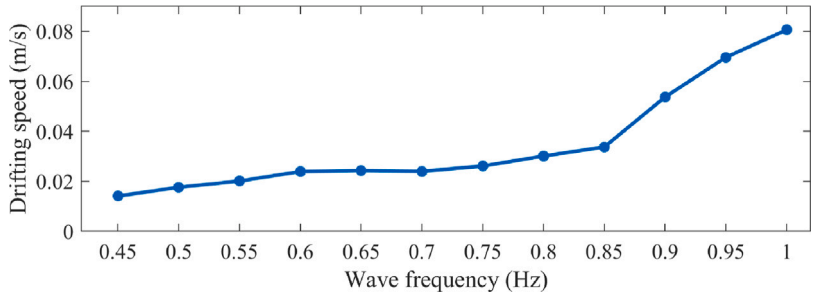

Fig. 12. The drifting speed under different wave frequency.

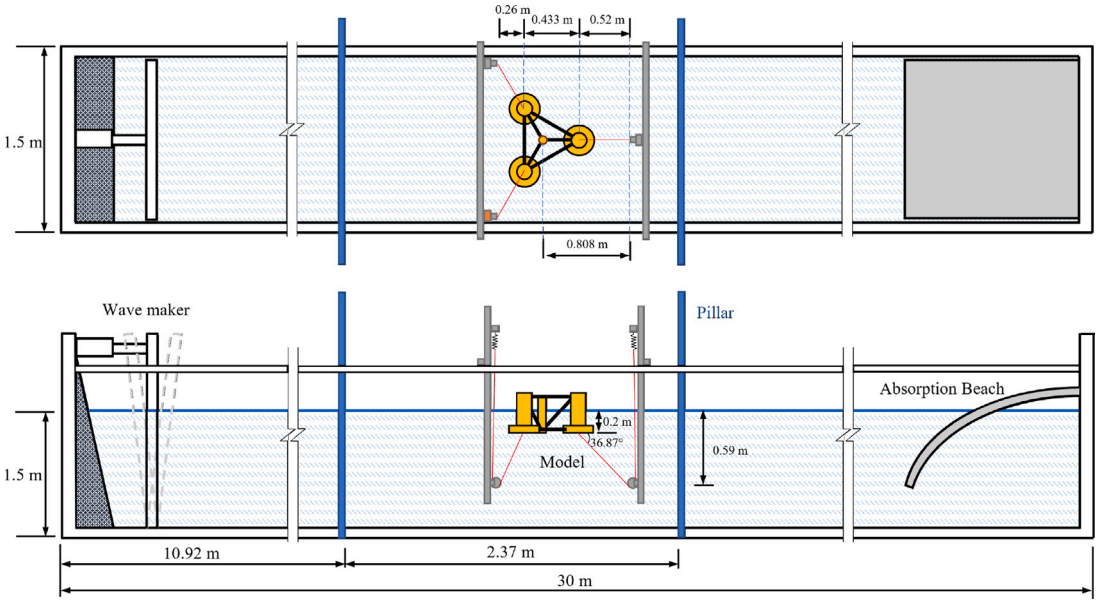

Fig. 13. Schematic diagram of the wave tank setup with mooring system.

columns and attached to the interconnecting beams. The setup features a front foil at a 30-degree pitch angle, with two vertically offset foils (see Fig. 5). This configuration is optimized based on previous findings.

The wave tank experiments utilized a complex mooring arrangement (Robertson et al., 2018), comprising five aluminum beams: two placed horizontally and three vertically. Pulleys were mounted on the vertical beams at a water depth of 0.59 m to facilitate the smooth movement of the mooring lines and to adjust the initial tension of the springs located above the water surface. High-strength fishing line, 0.50 mm in diameter and capable of withstanding forces up to 210 N, was employed as the mooring line material. One end of each line was anchored at the base of the platform's columns, while the other end, after being threaded through the pulleys, was connected to springs fixed at a consistent height above the water surface. This configuration ensured a stable orientation of the platform in calm water. The mooring system was strategically designed so that the lines were positioned at a 120° angle relative to each other, with each line forming an angle of 36.87° with the underwater horizontal plane. The force sensor mentioned before was installed on one of the front vertical aluminum beams to facilitate accurate force measurements. Figs. 13 and 14 present the schematic and a photograph of the wave tank with the no-foil platform in place, respectively. Fig. 13 illustrates the detailed schematic of the wave tank and mooring system configuration, while Fig. 14 provides a photographic view of the platform with the mooring system set up in the tank. The platform's setup and position in the tank remain consistent, whether or not the foils are installed.

4.2. Discussion and result

4.2.1. Regular wave

The experiments were carried out with a regular head wave frequency of 0.65 Hz, varying the wave height to assess the adaptability of WDP under a range of wave conditions. The wave heights were methodically altered from 0.02 m to 0.20 m, in 0.02 m increments, to evaluate platform response and mooring line loads under varying environmental conditions, from mild to severe, which correspond to 2 m and 20 m wave heights in the full scale. Additionally, the condition with a wave height of 0.15 m was measured separately to ensure consistency, as previous measurements also utilized a 0.15 m wave height. Fig. 15 displays the average peak-to-peak amplitude of mooring loads under various wave heights, comparing scenarios with and without the integration of foils. The peak-to-peak tension amplitude – averaging the extremes in each motion cycle – serves as a pivotal indicator of platform stability and resilience. Consistent with theoretical expectations, an increase in mooring load correlates with escalating wave height, attributable to the augmented energy of larger waves. Moreover, the mooring loads recorded with the addition of foils are consistently lower than those without, demonstrating a significant and systematic reduction in loads when foils are employed. This discrepancy is particularly pronounced in the wave height range from 0.06 m to 0.10 m, where the difference in loads – referred to as the 'gap' in the figure – is more distinct. At a wave height of 0.10 m, the foils facilitate a remarkable 41.07% decrease in mooring tension. This pronounced reduction highlights the foils'

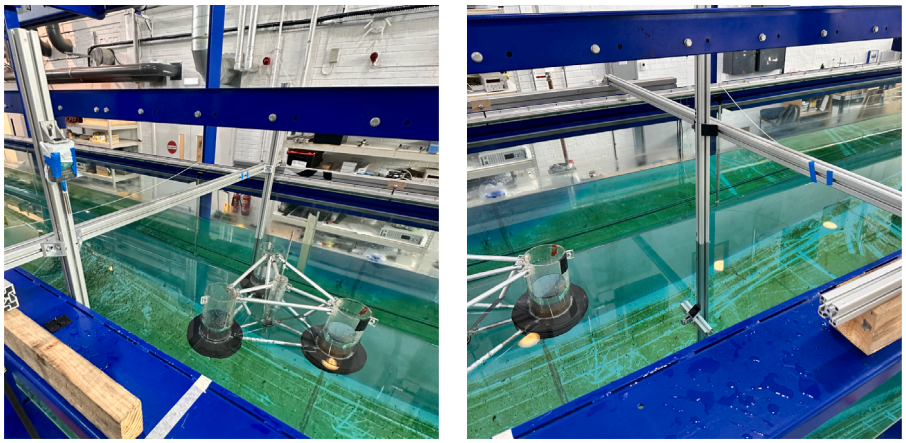

Fig. 14. Photograph of the platform with mooring system placed in the wave tank.

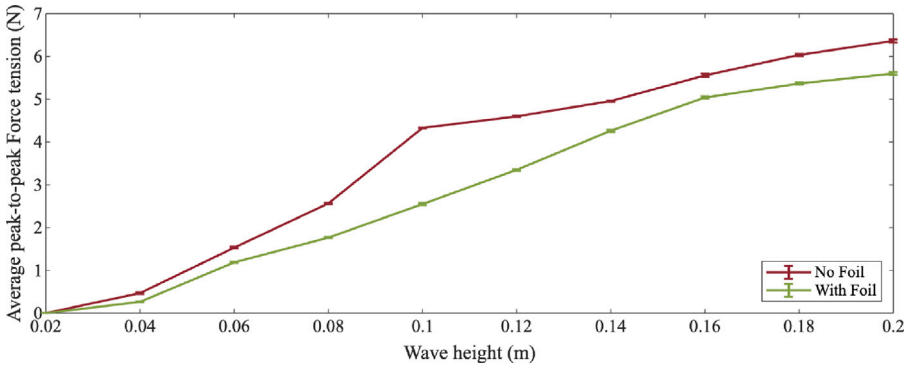

Fig. 15. Mooring load under various wave height: no foil vs. with foil.

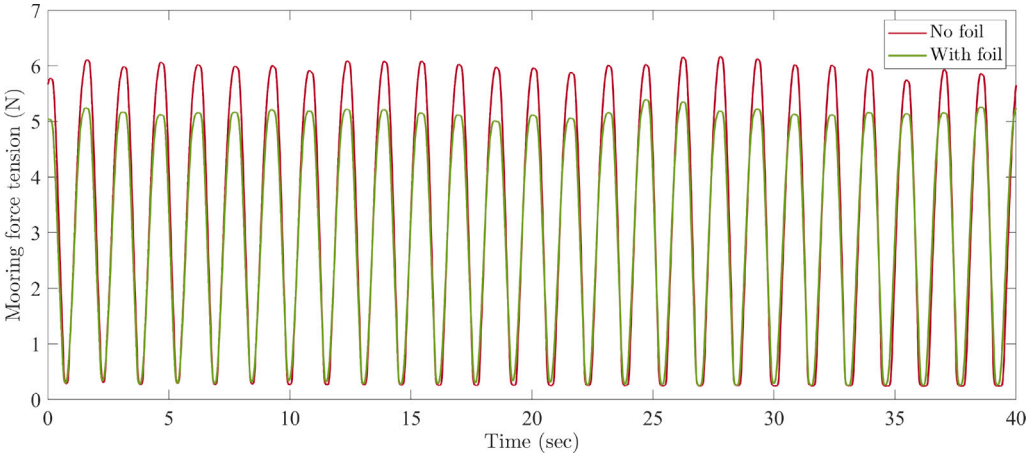

Fig. 16. Comparison of mooring load fluctuations over time without foil (red) versus with foil (green) under a constant wave frequency of 0.65 Hz and a wave height of 0.15 m.

efficacy in stabilizing the platform, particularly within this wave height range, providing critical insight into their operational performance and advantageous application conditions.

Given that the previous studies focused on a wave scenario characterized by a frequency of 0.65 Hz and a wave height of 0.15 m, this section examines this specific condition to investigate the changes in mooring tension over time. Fig. 16 illustrates the temporal variations in mooring load under a wave frequency of 0.65 Hz and a wave height of 0.15 m. The comparison between scenarios with (green line) and without (red line) a foil reveals significant insights. The periodicity of the load oscillations, approximately 1.54 s, is consistent with the wave period, which affirms the dominant role of wave motion in influencing the platform's dynamics. Additionally, the integration of the foil results in a marked 14.50% reduction in the mooring loads, which underscores its effectiveness in dampening wave-induced forces. This attenuation of peak loads indicates that the maximum stresses on the mooring system are alleviated, potentially enhancing the system's maintenance profile and extending its operational lifespan.

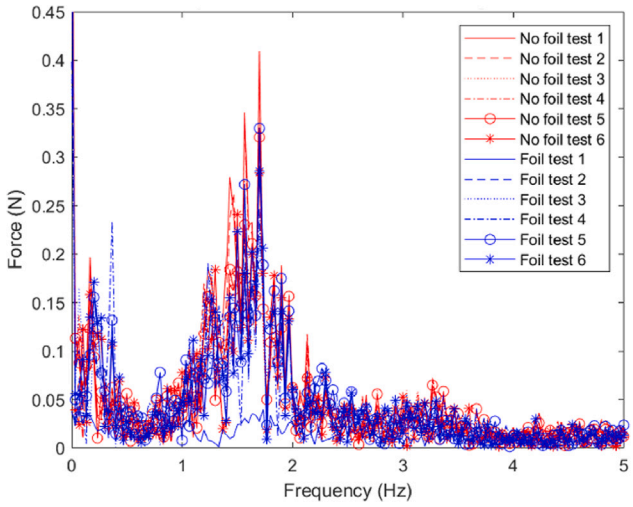

Fig. 17. Peak-to-peak variance in mooring line loads with and without a foil.

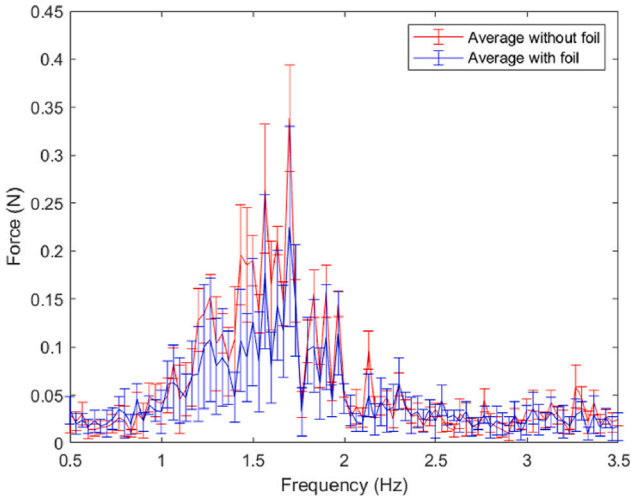

Fig. 18. Average variance in mooring line loads with and without a foil.

4.2.2. Irregular wave

The irregular JONSWAP-scaled wave conditions used in the experiment were characterized by significant wave height H_s = 0.125 m, peak period T_s = 1.253 s, and shape parameter γ = 3.3. Each test for mooring line loads was repeated six times to minimize errors and ensure consistency across results. The mooring line loads were recorded using load cells, with data collected for a duration of 90 s. Due to the irregular nature of the wave conditions, peak-to-peak mooring line loads cannot be directly referenced. Therefore, the force data will be analyzed using Fast Fourier Transform (FFT) to determine the frequency response, which represents the energy distribution over the specified time range.

The mooring line loads were analyzed in two primary ways: first, by examining the peak-to-peak mooring line loads with and without the foil; second, by calculating the average mooring line loads across all data sets. Figs. 17 and 18 illustrate these comparisons.

Fig. 17 presents the peak-to-peak mooring line load variance, demonstrating a reduction of 19.32% when the foil was attached to the platform. This decrease indicates that the foil effectively reduces dynamic load fluctuations by dampening the platform's response to irregular waves, thus mitigating extreme stress conditions that can occur during harsh wave events. By reducing these peak loads, the foil helps decrease the risk of structural failure in the mooring system, thereby improving the reliability of the platform.

Fig. 18 shows the average mooring line loads for all six tests. The addition of the foil resulted in a significant reduction of 33.3% in average loads. This demonstrates that, on average, the foil effectively reduces the force acting on the mooring lines. This is likely due to the foil's ability to stabilize the platform and reduce oscillatory motion caused by irregular waves. This reduction not only contributes to a more consistent load distribution over time but also helps to minimize fatigue in the mooring system, leading to an extended service life of the components.

5. Conclusion

This paper highlights an advancement in offshore wind energy, focusing on the application of foil-induced Wave Devouring Propulsion (WDP) for semi-submersible Floating Offshore Wind Turbine (FOWT) platforms to improve stability. It investigated the effects of foils on drift speed, heave motion, and mooring line tension in dynamic wave conditions, using a free-floating/moored platform with various foil configurations. The study examined foil angles, wave period, and amplitude conditions, providing important insights for optimizing platform-with-foil designs.

The experimental results showed significant reductions in platform drift and mooring line tension, with a reduction of up to 41.07% in mooring tension at a wave height of 0.10 m and a frequency of 0.65 Hz. These results are supported by a detailed analysis of the WDP mechanism, which explains how foils effectively convert wave energy into propulsion forces to mitigate the platform's dynamic response.

The core mechanism lies in the interaction between the foils and the surrounding fluid, where the foils generate wake patterns depending on their movement relative to the waves. Under optimal conditions, a reversed von Kármán vortex street (RvK) forms in their wake, accelerating the flow behind the foils. This acceleration reduces the drag acting on the platform and provides a forward thrust force that counteracts wave-induced drift. Unlike conventional stabilization methods that rely on external energy, WDP passively converts wave energy, turning it into thrust to maintain platform stability.

This passive stabilization reduces both platform drift and mooring line loads, demonstrating WDP's ability to mitigate surge and sway responses that are challenging for offshore platforms. Moreover, the experimental observations reveal that the foils act as energy dampers, converting wave-induced oscillations into controlled movements, generating stabilizing forces. This mechanism minimizes the need for active stabilization and highlights the potential of WDP to extend the lifespan of the platform's mooring system by reducing fatigue loads.

In addition, we explored various foil configurations and identified that a combination of one frontal foil with a pitch angle of 30° and two vertical foils provided optimal performance. This configuration effectively balances thrust generation and drag reduction, ensuring the platform remains stable even under adverse wave conditions. The enhanced stability provided by the foils reduces platform movement and structural stresses, improving the safety and reliability of wind turbine operations.

Although this study demonstrates promising potential for WDP, several limitations must be acknowledged. The environmental conditions considered were idealized, involving only regular and typical irregular waves, and assuming a single flow direction, effectively reducing the complexity to a quasi-three-dimensional experiment. Additionally, the foils were fixed and only allowed to passively respond to waves with platform motion, without exploring active control, which has been shown to enhance thrust generation. The impact of foil material was not considered, nor were other foil shapes beyond NACA 0030, such as NACA 0012, NACA 0015, or flat plates, which could yield different performance characteristics. These limitations underscore the exploratory

nature of this research, serving as a starting point for further studies under more realistic conditions and configurations.

The insights gained from this study underscore the significance of understanding the physical mechanisms behind WDP, emphasizing its potential as a sustainable and low-maintenance solution for floating offshore wind platforms. Future research should further investigate the effects of different foil materials, shapes, and dynamic behaviors under varying sea states to maximize the efficiency and adaptability of WDP across diverse marine environments.

CRediT authorship contribution statement

Jingru Xing: Writing – original draft, Visualization, Validation, Investigation, Formal analysis, Conceptualization. **Junxian Wang:** Formal analysis, Data curation, Conceptualization. **Ashkan Matin:** Data curation, Formal analysis. **Ninad Prashant Vaidya:** Data curation. **Liang Yang:** Writing – review & editing, Supervision, Resources, Project administration, Methodology, Funding acquisition. **Nicholas Townsend:** Writing – review & editing, Supervision. **Lei Zuo:** Writing – review & editing, Supervision, Conceptualization.

Declaration of competing interest

The authors declare that they have no known competing financial interests or personal relationships that could have appeared to influence the work reported in this paper.

Acknowledgments

Liang Yang acknowledges the support from the HEIF fund for the project 'Novel Floating Wind Platform', the Future Frontiers Fund (FFF) from Cranfield University and Cranfield Global Research Fund.

References

Alvik, S., 2023. Long journey south for levelised energy cost means offshore wind will weather the storm. URL https://www.rechargenews.com/energy-transition/long-journey-south-for-levelised-energy-cost-means-offshore-wind-will-weather-the-storm/2-1-1542794. (Accessed 18 February 2024).

Anderson, J.M., 1996. Vorticity Control for Efficient Propulsion (Ph.D. thesis). Massachusetts Institute of Technology.

Arany, L., Bhattacharya, S., Macdonald, J., Hogan, S.J., 2017. Design of monopiles for offshore wind turbines in 10 steps. Soil Dyn. Earthq. Eng. 92, 126–152.

Aryawan, I., McEvoy, P., Kim, S., Faria, R.P., 2023. Potential mooring system optimization using polymer spring component–floating offshore wind turbine application. In: Offshore Technology Conference. OTC, D031S032R001.

2023. Autonautusv. URL https://autonautusv.com/vessels-0. (Accessed 17 June 2023).

Bezunartea-Barrio, A., Fernandez-Ruano, S., Maron-Loureiro, A., Molinelli-Fernandez, E., Moreno-Buron, F., Oria-Escudero, J., Rios-Tubio, J., Soriano-Gomez, C., Valea-Peces, A., Lopez-Pavon, C., et al., 2020. Scale effects on heave plates for semi-submersible floating offshore wind turbines: case study with a solid plain plate. J. Offshore Mech. Arct. Eng. 142 (3), 031105.

Bjørneset, S., 2014. Modelling and Control of Thruster Assisted Position Mooring System for a Semi-submersible: Analysis and Model Testing (Master's thesis). Institutt for marin teknikk.

Bøckmann, E., Yrke, A., Steen, S., 2018. Fuel savings for a general cargo ship employing retractable bow foils. Appl. Ocean Res. 76, 1–10.

Bohl, D.G., Koochesfahani, M.M., 2009. MTV measurements of the vortical field in the wake of an airfoil oscillating at high reduced frequency. J. Fluid Mech. 620, 63–88.

Bowker, J.A., Tan, M., Townsend, N.C., 2020. Forward speed prediction of a free-running wave-propelled boat. IEEE J. Ocean. Eng. 46 (2), 402–413.

Bowker, J., Townsend, N., 2022. Evaluation of bow foils on ship delivered power in waves using model tests. Appl. Ocean Res. 123, 103148.

Bowker, J., Townsend, N., Tan, M., Shenoi, R., 2015. Experimental study of a wave energy scavenging system onboard autonomous surface vessels (ASVs). In: OCEANS 2015-Genova. IEEE, pp. 1–9.

Bricheno, L.M., Wolf, J., Aldridge, J., 2015. Distribution of natural disturbance due to wave and tidal bed currents around the UK. Cont. Shelf Res. 109, 67–77.

Chan, C., Wang, J., Yang, L., Zang, J., 2024. Wave-assisted propulsion: An experimental study on traveling ships. Phys. Fluids 36 (2).

Chuang, T.-C., Yang, W.-H., Yang, R.-Y., 2021. Experimental and numerical study of a barge-type FOWT platform under wind and wave load. Ocean Eng. 230, 109015.

Du, A., 2021. Semi-submersible, spar and TLP – how to select floating wind foundation types? URL https://www.empireengineering.co.uk/semi-submersible-spar-and-tlp-floating-wind-foundations/. (Accessed 18 February 2024).

Hine, R., Willcox, S., Hine, G., Richardson, T., 2009. The wave glider: A wave-powered autonomous marine vehicle. In: OCEANS 2009. IEEE, pp. 1–6.

Ideol, B.W., 2022. Floatgen. https://www.bw-ideol.com/en/floatgen-demonstrator. (Accessed 18 February 2024).

Isshiki, H., Murakami, M., 1983. A theory of wave devouring propulsion (3rd report) an experimental verification of thrust generation by a passive-type hydrofoil propulsor. J. Soc. Nav. Archit. Jpn. 1983 (154), 118–128.

Isshiki, H., Murakami, M., 1984. A theory of wave devouring propulsion (4th report) a comparison between theory and experiment in case of a passive-type hydrofoil propulsor. J. Soc. Nav. Archit. Jpn. 1984 (156), 102–114.

Johnston, E., 2018. FOWT 2018 presentation. Available online URL https://uploads-ssl.webflow.com/5f8964a5a533790d6cc8820a/5f96cb79cdb542f472ddef2a_3_FOWT-2018-full-Eve-Johnston.pdf. (Accessed 18 February 2024).

Johnston, P., Poole, M., 2017. Marine surveillance capabilities of the AutoNaut wave-propelled unmanned surface vessel (USV). In: OCEANS 2017-Aberdeen. IEEE, pp. 1–46.

Lagopoulos, N., Weymouth, G., Ganapathisubramani, B., 2019. Universal scaling law for drag-to-thrust wake transition in flapping foils. J. Fluid Mech. 872.

Lopez-Pavon, C., Souto-Iglesias, A., 2015. Hydrodynamic coefficients and pressure loads on heave plates for semi-submersible floating offshore wind turbines: A comparative analysis using large scale models. Renew. Energy 81, 864–881.

Ma, K.-T., Luo, Y., Kwan, C.-T.T., Wu, Y., 2019. Mooring System Engineering for Offshore Structures. Gulf Professional Publishing.

Ramamurti, R., Sandberg, W., 2001. Computational study of 3-D flapping foil flows. In: 39th Aerospace Sciences Meeting and Exhibit. p. 605.

Read, D.A., Hover, F., Triantafyllou, M., 2003. Forces on oscillating foils for propulsion and maneuvering. J. Fluids Struct. 17 (1), 163–183.

Robertson, A.N., Bachynski, E.E., Gueydon, S., Wendt, F., nemann, P.S., Jonkman, J., 2018. Assessment of experimental uncertainty for a floating wind semisubmersible under hydrodynamic loading. In: International Conference on Offshore Mechanics and Arctic Engineering. Vol. 51319, V010T09A076.

Robertson, A.N., Wendt, F., Jonkman, J.M., Popko, W., Dagher, H., Gueydon, S., Qvist, J., Vittori, F., Azcona, J., Uzunoglu, E., et al., 2017. OC5 project phase II: validation of global loads of the DeepCwind floating semisubmersible wind turbine. Energy Procedia 137, 38–57.

Roddier, D., Cermelli, C., Aubault, A., Weinstein, A., 2010. WindFloat: A floating foundation for offshore wind turbines. J. Renew. Sustain. Energy 2 (3).

Streitlien, K., Triantafyllou, G., 1998. On thrust estimates for flapping foils. J. Fluids Struct. 12 (1), 47–55.

Tan, L., Ikoma, T., Aida, Y., Masuda, K., 2021. Mean wave drift forces on a barge-type floating wind turbine platform with moonpools. J. Mar. Sci. Eng. 9 (7), 709.

Terao, Y., 2009. Wave devouring propulsion system: From concept to trans-pacific voyage. In: International Conference on Offshore Mechanics and Arctic Engineering. Vol. 43444, pp. 119–126.

Triantafyllou, M., Triantafyllou, G., Gopalkrishnan, R., 1991. Wake mechanics for thrust generation in oscillating foils. Phys. Fluids A 3 (12), 2835–2837.

Wang, J., Santhosh, S., Colomés, O., Capaldo, M., Yang, L., 2023. Experimental study of dynamic response of passive flapping hydrofoil in regular wave. Phys. Fluids 35 (7).

Wang, J., Xing, J., Siddiqui, M.S., Stawiarska, A., Yang, L., 2024. Experimental investigation of wave induced flapping foil for marine propulsion: Heave and pitch stiffness effect. J. Renew. Sustain. Energy 16 (2).

Weinblum, G.P., 1954. Approximate theory of heaving and pitching of hydrofoils in regular shallow waves. David W Taylor Model Basin, Navy Department, Report C-479, Hydromechanics Laboratory, Research and Development Report.

WindEurope, 2017. Floating offshore wind vision statement. URL https://windeurope.org/wp-content/uploads/files/about-wind/reports/Floating-offshore-statement.pdf, WindEurope.

Wu, X., Zhang, X., Tian, X., Li, X., Lu, W., 2020. A review on fluid dynamics of flapping foils. Ocean Eng. 195, 106712.

Xing, J., Stagonas, D., Hart, P., Zhang, C., Yang, J., Yang, L., 2024. Numerical investigation of wave induced thrust on a submerged hydrofoil. J. Renew. Sustain. Energy 16 (5).

Xing, J., Yang, L., 2023. Wave devouring propulsion: An overview of flapping foil propulsion technology. Renew. Sustain. Energy Rev. 184, 113589.

Yang, J., He, E., Hu, Y., 2019. Dynamic modeling and vibration suppression for an offshore wind turbine with a tuned mass damper in floating platform. Appl. Ocean Res. 83, 21–29.

Yoshida, H., Yamasaki, K., Sunahara, S., 2018. Application of wave devouring propulsion technology to support positioning of floating structure. In: International Conference on Offshore Mechanics and Arctic Engineering. Vol. 51203, American Society of Mechanical Engineers, V001T01A024.

Yu, W., Lemmer, F., Cheng, P.W., 2023. Modeling and validation of a tuned liquid multi-column damper stabilized floating offshore wind turbine coupled system. Ocean Eng. 280, 114442.